

1 **Comment on “Origin of water in the Badain Jaran Desert, China:**
2 **new insight from isotopes” by Wu et al. (2017)**

3 **Lucheng Zhan¹, Jiansheng Chen², Ling Li³ and D. A. Barry⁴**

4 ¹ State Key Laboratory of Hydrology-Water Resources and Hydraulic Engineering, Hohai
5 University, Nanjing, 210098, China

6 ² College of Earth Sciences and Engineering, Hohai University, Nanjing, 210098, China

7 ³ School of Civil Engineering, the University of Queensland, St. Lucia, QLD 4072, Australia

8 ⁴ Laboratoire de technologie écologique (ECOL), Institut d’ingénierie de l’environnement (IIE),
9 Faculté de l’environnement naturel, architectural et construit (ENAC), Ecole Polytechnique
10 Fédérale de Lausanne (EPFL), Station 2, 1015 Lausanne, Switzerland

11 *Correspondence to:* Jiansheng Chen (jschen@hhu.edu.cn)

12 **Abstract**

13 Precipitation isotope data were used to determine the origin of groundwater in the Badain Jaran
14 Desert (BJD) in the study of Wu et al. (2017). Both precipitation and its isotope composition
15 vary seasonally, so arithmetic averages of precipitation isotope values poorly represent the
16 isotope composition of meteoric water. Their finding that the BJD groundwater is recharged by
17 modern meteoric water from local areas including the southeastern adjacent mountains was
18 based on arithmetic averaging. However, this conclusion is not supported by the corrected mean
19 precipitation isotope values, which are weighted by the precipitation rate. Indeed, the available
20 isotopic evidence shows that modern precipitation on the Qilian Mountains is more likely to be
21 the main source of the groundwater and lake water in the BJD, as found by Chen et al. (2004).

22 **1 Introduction**

23 The Badain Jaran Desert (BJD) is characterized by a unique landscape that contains a large
24 number of lakes and the world's largest stationary sand dunes maintained by groundwater (Chen
25 et al., 2004). However, the origin of the groundwater remains uncertain (Dong et al., 2013).
26 Using stable and radioactive environmental isotopes, Wu et al. (2017) investigated the
27 connection between lakes and groundwater, and the origin of groundwater in the southeastern
28 desert area. They suggested that the BJD groundwater is derived primarily from modern
29 meteoric water from local areas, including the southeastern adjacent small mountains. Based
30 on isotopic evidence, the authors ruled out other hypotheses on the groundwater source,
31 including fossil groundwater (Gates et al., 2008; Ma and Edmunds, 2006; Wang et al., 2015;
32 Yang et al., 2010) and snowmelt from the Qilian Mountains, 500 km (center-to-center distance)
33 southwest of the desert (Chen et al., 2004; 2006).

34 The authors argued that the ^{14}C dating over-estimated the age (~10 ka) of the BJD
35 groundwater due to interference by additional dead carbon input from ancient carbonates. We
36 have conducted work related to the ^{14}C dating and found the same problem with overestimation
37 of the groundwater age (Chen et al., 2014; Wang and Chen, 2018). Wu et al. (2017) reasoned
38 that the average age of groundwater in the BJD should be much younger, since it includes
39 modern meteoric water as indicated by tritium levels (Gates et al., 2008; Wu et al., 2017). They

40 presented many evidences and discussions for their conclusion of groundwater recharged by
41 modern precipitation from local areas. However, their averaging of the precipitation isotope
42 data did not account for seasonality of precipitation amount, which led to a misconception of
43 the potential groundwater origin.

44 **2 Source water identification based on weighted mean precipitation isotope values**

45 The determination of mean precipitation isotope values is of great significance for assessing the
46 contribution of precipitation as a water source to regional hydrological systems and for
47 assessing interactions among different hydrological components. To examine the relationship
48 between the BJD groundwater and local precipitation, historical precipitation isotope data from
49 a nearby GNIP (Global Network of Isotopes in Precipitation,
50 <https://nucleus.iaea.org/wiser/index.aspx>) station in Zhangye (1986–2003) were used by Wu et
51 al. (2017). The GNIP database provides data on monthly precipitation isotopes as well as
52 monthly rainfall for the Zhangye station. As shown in Figure 1a, b, the monthly δD and $\delta^{18}O$
53 values in the study area exhibit large seasonal variations, which are mainly controlled by
54 temperature (Zhan et al., 2017). The isotopic seasonality pattern of precipitation is similar in
55 different years. During the summer half year when temperature is higher, the rainfall is more
56 enriched in heavier isotopes.

57 According to the GNIP data, the mean annual precipitation is about 130 mm, with more
58 than 60% of the total annual rainfall occurring from June to August during which the isotope
59 values are the highest (Figure 1b). Since the annual precipitation is seasonal, the monthly
60 precipitation isotope data should be weighted by the monthly precipitation amount to calculate
61 the annual mean for representing the isotope composition of local precipitation as a potential
62 source of the BJD groundwater. The weighted mean isotopic values $\overline{\delta}_w$ can be calculated
63 using:

$$64 \quad \overline{\delta}_w = \frac{\sum_{j=Jan}^{Dec} \overline{\delta}_j \cdot \overline{P}_j}{\sum_{j=Jan}^{Dec} \overline{P}_j} \quad (1)$$

65 where $\overline{\delta}_j$ and \overline{P}_j are the averaged isotopic values and averaged rainfall amount of month j
 66 during the GNIP observation years, respectively. The monthly averages, $\overline{\delta}_j$ and \overline{P}_j can be
 67 calculated as follows:

$$68 \quad \overline{\delta}_j = \frac{\sum_i \delta_{i,j}}{n} \quad (2)$$

$$69 \quad \overline{P}_j = \frac{\sum_i P_{i,j}}{n} \quad (3)$$

70 where $\delta_{i,j}$ and $P_{i,j}$ are the isotopic value (δD or $\delta^{18}O$) and rainfall amount of month j in
 71 year i from the available GNIP dataset, respectively; and n is the corresponding number of
 72 available data.

73 Based on the dataset from the GNIP database, the calculated weighted mean values for δD
 74 and $\delta^{18}O$ of Zhangye's precipitation are -40.9‰ and -5.50‰, respectively (Figure 1c). Using
 75 arithmetic averages, Wu et al. (2017) determined δD and $\delta^{18}O$ values around -74‰ and -10.5‰,
 76 respectively. When plotted on the $\delta^{18}O$ - δD graph (Figure 1c), the arithmetic average values are
 77 close to the intersection of the evaporation line EL1 (for groundwater and lake water in the
 78 desert) and the GMWL (Global Meteoric Water Line), which led Wu et al. (2017) to conclude
 79 that groundwater and lake water in the BJD originates from modern meteoric precipitation in
 80 local areas including the adjacent small mountains. However, if the weighted mean values are
 81 used, this conclusion no longer holds. Compared with the isotope composition of the local
 82 precipitation, the source water recharging the BJD groundwater and lakes is much more
 83 depleted in D and ^{18}O .

84 **3 Reanalysis on the origin of groundwater in the BJD**

85 Using available data from literature, we reanalyzed the possible origin of groundwater in the
 86 BJD. We focus on the BJD southern margin area where the desert lakes are mostly concentrated.
 87 The isotope data of the groundwater and lake water (Figure 2a) lie on the evaporation line EL2
 88 ($\delta D = 4.6\delta^{18}O - 29.8$, $r^2 = 0.94$), which is reasonably similar to EL1 in Wu et al. (2017). Here

89 only data from groundwater and lake water samples within the BJD area were used for
90 determining the EL2. The weighted mean isotope values of precipitation in the regions close to
91 the BJD (blue circles) show a decreasing trend with increasing elevation from 1382 to 2569 m
92 a.s.l., reflecting the effect of elevation on isotope fractionation (Poage and Chamberlain, 2001).
93 The intersection of EL2 and GMWL ($\delta D = -83.6\text{‰}$, $\delta^{18}O = -11.7\text{‰}$), which represents the mean
94 isotope composition of the recharge source for BJD groundwater, is outside the range of
95 precipitation in the local and adjacent regions, indicating another different source water with
96 more depleted isotope composition.

97 Together with the statistical isotopic values of precipitation in the BJD and the Qilian
98 Mountains (rainfall and snowmelt) from literature data, a significant inverse correlation of δD
99 and $\delta^{18}O$ values with elevation of the precipitation can be established (Figure 2b, c). The altitude
100 gradients for δD and $\delta^{18}O$ are $-2.0\text{‰}/100\text{m}$ and $-0.26\text{‰}/100\text{m}$, respectively, which are close to
101 global mean levels (Poage and Chamberlain, 2001). Based on these gradients, the location of
102 water associated with the intersection of EL2 and GMWL corresponds to an average elevation
103 of 3914 m a.s.l. (3920 m estimated by δD and 3908 m by $\delta^{18}O$). Therefore, the recharge region
104 for groundwater and lake water in the BJD is likely to include areas of elevations higher than
105 3914 m a.s.l. to produce source water of more depleted isotope composition.

106 The closest region that could meet this elevation requirement is the Qilian Mountains
107 (average elevation between 4000 and 5000 m a.s.l.), northeast of the Qinghai-Tibet Plateau
108 (Figure 3a). Nineteen snowmelt and rainfall water samples from 3540 to 5010 m a.s.l. in the
109 glacier zone of the Qilian Mountains were collected by Ren (1999). The statistical isotope
110 compositions of these samples are close to that given by the GMWL-EL2 intersection (Figure
111 2a). Therefore, the isotope evidence points to the Qilian Mountains as a main source region for
112 groundwater and lake water in the BJD, as observed previously (Chen et al., 2004).

113 Wu et al. (2017) ruled out the Qilian Mountains as a recharge area for groundwater in the
114 BJD based on the large isotopic difference between the GMWL-EL2 intersection and data from
115 water samples mainly collected from the Shiyang River watershed (Li et al., 2016), which is
116 located in the eastern lower area of the Qilian Mountains. The mean elevation of the Shiyang
117 River watershed is only 2487 m a.s.l. (Bourque and Hassan, 2009), which is lower than the

118 mean elevation of the entire mountain. Therefore, their argument for excluding the Qilian
119 Mountains as a recharge region is questionable. Water samples collected from rivers on the
120 northern slope of the Qilian Mountains are characterized by large variations of isotope
121 compositions (Figure 2a), with the lowest isotopic values found by Ren (1999) from a river in
122 the upstream glacier zone. Scattered data between the plots of snowmelt on the mountain and
123 rainfall in lower regions indicated that most of these river samples are likely to be mixtures of
124 snowmelt water and piedmont precipitation. Isotope signatures show little connection between
125 these rivers on the northern slope and the groundwater in the BJD.

126 The relationship between d-excess and $\delta^{18}\text{O}$ was also discussed by Wu et al. (2017). The
127 d-excess value ($\text{d-excess} = \delta\text{D} - 8\delta^{18}\text{O} < 0$) indicates the deviation from the GMWL, reflecting
128 the degree of evaporation experienced by the available water. Wu et al. (2017) noted the
129 difference in the d-excess value between the Qilian-sourced water (sampled from the northern
130 slope rivers of the Qilian Mountains region) and BJD groundwater, and argued that the Qilian
131 Mountains cannot be the origin of the latter because no evaporation could occur to water
132 underground. Located in the northeastern margin of the Qinghai-Tibet Plateau, the Qilian
133 Mountains area consists of many northwest–southeast parallel mountain ranges and valleys
134 (Qiu et al., 2016). Although little evidence of evaporation was found in sampled river water
135 from the northern slope area, water in other near-surface water systems (like lakes, wetlands,
136 and soil water reservoir) of longer residence time within the wide Qilian Mountains region
137 would have been subjected to more intense evaporation and produced isotopic signatures
138 similar to that of the BJD groundwater. The d-excess results cannot exclude the Qilian
139 Mountains as a recharge region either.

140 Groundwater in the BJD has also been postulated to be sourced from the Yabulai Mountain
141 region (Figure 3a). The highest mountain there is 1938 m a.s.l., which is unlikely to provide
142 rainfall input with depleted heavy isotopes as shown in Figure 2. In a recent groundwater
143 resource development project, eight wells were drilled (depths of 135 to 260 m) in the
144 southeastern part of the BJD. The static groundwater levels in these wells show a decreasing
145 trend from southwest to northeast (Figure 3b), indicating an overall movement of groundwater
146 along this direction. The groundwater flow direction is consistent with our hypothesis that BJD

147 groundwater originates from the Qilian Mountains (located southwest of the BJD). Researchers
148 have also examined the chemistry of lake water and groundwater in the study area and
149 surrounding areas. For example, Yang and Williams (2003) investigated the ion chemistry of
150 lake water and groundwater from the BJD and its periphery, and ruled out the possibility of
151 recharge from recent local rainfall to the lakes and groundwater. In a previous study (Chen et
152 al., 2012), the hydrochemical and isotopic results also supported our remote recharge
153 hypothesis.

154 We agree with the concern of Wu et al. (2017) on the accuracy of ^{14}C dating for the BJD
155 groundwater, which provided estimates of very old ages. Recent work (Wang and Chen, 2018)
156 found considerable overestimation of the groundwater age by the ^{14}C dating method due to
157 neglect of dead carbon brought by deep CO_2 emission. In contrast to the fossil groundwater
158 hypothesis, the detectable tritium activities as shown by Wu et al. (2017) and many others (Chen
159 et al., 2006; Gates et al., 2008; Yang and Williams, 2003) indicate a modern precipitation source
160 of the BJD groundwater. This suggests that the Qilian Mountains-sourced groundwater flows
161 through hundreds of kilometers over only tens of years. We suggest that, due to geological
162 activities, various southwest–northeast deep fault systems exist between the Qilian Mountains
163 and the desert (Chen et al., 2006). Based on the geological conditions and geochemical
164 evidences (helium results), these large deep fault systems are hypothesized to act as a quick
165 passage for the groundwater (Chen et al., 2006, 2004, 2012), which explains the detectable
166 tritium in the groundwater.

167 The reanalysis above supports the hypothesis that groundwater in the BJD mainly
168 originates from modern precipitation of Qilian Mountains. Near-surface water in the Qilian
169 Mountains, subjected to evaporation, infiltrates and recharges groundwater, which is then
170 delivered to the BJD through the deep interconnected faults. Of course, more work is needed to
171 support this hypothesis conclusively. It should also be noted that, the higher average elevation
172 (4000 to 5000 m a.s.l.) of the Qilian Mountains than the estimated mean recharge elevation
173 (3914 m a.s.l.) estimated in this study, as well as the large variation of isotope composition of
174 groundwater in the BJD, may imply a mixture of the Qilian-sourced water (of more depleted
175 isotope composition from 4000 to 5000 m a.s.l) with precipitation from other lower areas.

176 Groundwater might have mixed with rainwater from low-elevation areas on its pathway.

177 **4 Concluding remarks**

178 We reanalyzed the precipitation isotope data of the Zhangye station to determine the original
179 source of the groundwater in the Badain Jaran Desert. These data were averaged arithmetically
180 in the recent study of Wu et al. (2017), whereas weighted averaging is more appropriate. The
181 reanalysis does not support the conclusion of Wu et al. (2017) that the BJD groundwater is
182 sourced from local meteoric water. Indeed, the reanalysis suggests a mean recharge elevation
183 of about 3914 m a.s.l. for the BJD groundwater, which indicates that the precipitation in the
184 Qilian Mountains region is a more likely main source of the BJD groundwater, as initially
185 hypothesized by Chen et al. (2004).

186 **References**

- 187 Bourque, C. P. A. and Hassan, Q. K.: Vegetation control in the long-term self-stabilization of
188 the Liangzhou Oasis of the Upper Shiyang River watershed of west-central Gansu,
189 Northwest China, *Earth Interact.*, 13(13), 1–22, doi:10.1175/2009EI286.1, 2009.
- 190 Chen, J., Zhao, X., Sheng, X., Dong, H., Rao, W. and Su, Z.: Formation mechanisms of
191 megadunes and lakes in the Badain Jaran Desert, Inner Mongolia, *Chinese Sci. Bull.*,
192 51(24), 3026–3034, doi:10.1007/s11434-006-2196-8, 2006.
- 193 Chen, J. S., Li, L., Wang, J. Y., Barry, D. A., Sheng, X. F., Zu Gu, W., Zhao, X. and Chen, L.:
194 Groundwater maintains dune landscape, *Nature*, 432(7016), 459–460,
195 doi:10.1038/nature03166, 2004.
- 196 Chen, J. S., Sun, X. X., Gu, W. Z., Tan, H. B., Rao, W. B., Dong, H. Z., Liu, X. Y. and Su, Z.
197 G.: Isotopic and hydrochemical data to restrict the origin of the groundwater in the Badain
198 Jaran Desert, Northern China, *Geochem. Int.*, 50(5), 455–465,
199 doi:10.1134/S0016702912030044, 2012.
- 200 Chen, X., Chen, J. and Wang, T.: A discussion of groundwater dating in Northern China, *Water*
201 *Resour. Prot.*, 30(2), 1–5, doi:10.3969/j.issn.1004-6933.2014.02.001, 2014.
- 202 Dong, Z., Qian, G., Lv, P. and Hu, G.: Investigation of the sand sea with the tallest dunes on

203 Earth: China's Badain Jaran Sand Sea, *Earth-Science Rev.*, 120(322), 20–39,
204 doi:10.1016/j.earscirev.2013.02.003, 2013.

205 Gates, J. B., Edmunds, W. M., Darling, W. G., Ma, J., Pang, Z. and Young, A. A.: Conceptual
206 model of recharge to southeastern Badain Jaran Desert groundwater and lakes from
207 environmental tracers, *Appl. Geochem.*, 23(12), 3519–3534,
208 doi:10.1016/j.apgeochem.2008.07.019, 2008.

209 Li, Z., Qi, F., Wang, Q. J., Song, Y., Aifang, C. and Jianguo, L.: Contribution from frozen soil
210 meltwater to runoff in an in-land river basin under water scarcity by isotopic tracing in
211 northwestern China, *Glob. Planet. Change*, 136, 41–51,
212 doi:10.1016/j.gloplacha.2015.12.002, 2016.

213 Ma, J. and Edmunds, W. M.: Groundwater and lake evolution in the Badain Jaran Desert
214 ecosystem, Inner Mongolia, *Hydrogeol. J.*, 14(7), 1231–1243, doi:10.1007/s10040-006-
215 0045-0, 2006.

216 Poage, M. A. and Chamberlain, C. P.: Empirical relationships between elevation and the stable
217 isotope composition of precipitation and surface waters: Considerations for studies of
218 paleoelevation change, *Am. J. Sci.*, 301(1), 1–15, doi:10.2475/ajs.301.1.1, 2001.

219 Qiu, X., Zhang, M. and Wang, S.: Preliminary research on hydrogen and oxygen stable isotope
220 characteristics of different water bodies in the Qilian Mountains, northwestern Tibetan
221 Plateau, *Environ. Earth Sci.*, 75(23), 1491, doi:10.1007/s12665-016-6299-5, 2016.

222 Ren, J.: A study of chemical characteristics of snow, precipitation and surface water in the basin
223 of the glacier No. 29 in Danghe Nanshan, Qilian Mountains, *J. Glaciol. Geocryol.*, 21(2),
224 151–154, 1999.

225 Wang, F., Sun, D., Chen, F., Bloemendal, J., Guo, F., Li, Z., Zhang, Y., Li, B. and Wang, X.:
226 Formation and evolution of the Badain Jaran Desert, North China, as revealed by a drill
227 core from the desert centre and by geological survey, *Palaeogeogr. Palaeoclimatol.*
228 *Palaeoecol.*, 426, 139–158, doi:10.1016/j.palaeo.2015.03.011, 2015.

229 Wang, T. and Chen, J.: Overestimated groundwater 14 C ages triggered an inexpediency of
230 water policy in China, *Curr. Sci.*, 114, 1–4, doi:10.18520/cs/v114/i08/1751-1755, 2018.

231 Wu, J., Ding, Y., Ye, B., Yang, Q., Zhang, X. and Wang, J.: Spatio-temporal variation of stable
232 isotopes in precipitation in the Heihe River Basin, Northwestern China, *Environ. Earth*

233 Sci., 61(6), 1123–1134, doi:10.1007/s12665-009-0432-7, 2010.

234 Wu, X., Wang, X.-S., Wang, Y. and Hu, B. X.: Origin of water in the Badain Jaran Desert,
235 China: New insight from isotopes, *Hydrol. Earth Syst. Sci.*, 21(9), 4419–4431,
236 doi:10.5194/hess-21-4419-2017, 2017.

237 Yang, X. and Williams, M. A. J.: The ion chemistry of lakes and late Holocene desiccation in
238 the Badain Jaran Desert, Inner Mongolia, China, *Catena*, 51(1), 45–60,
239 doi:10.1016/S0341-8162(02)00088-7, 2003.

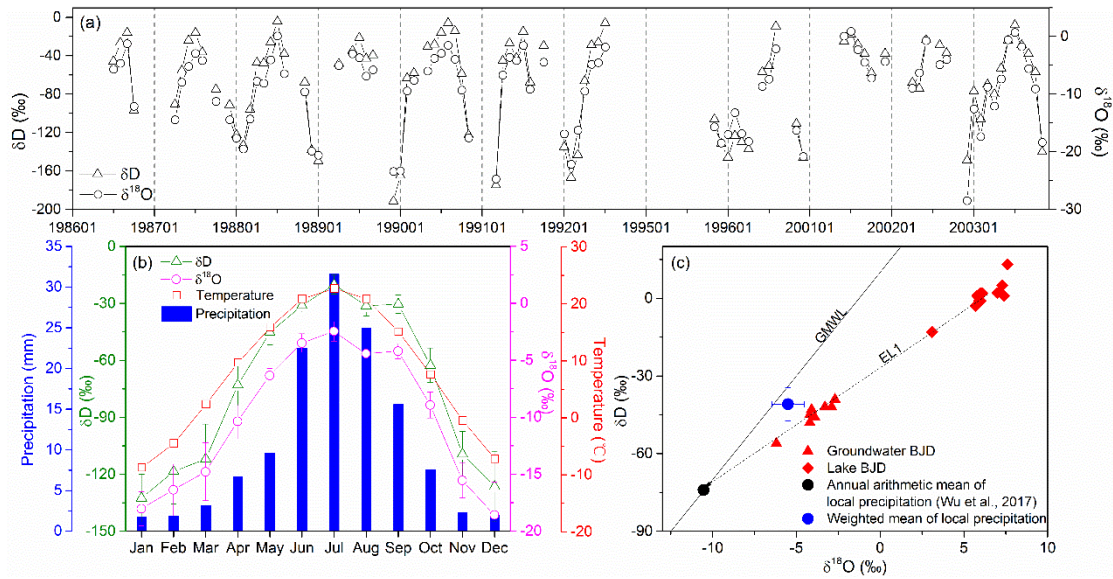
240 Yang, X., Ma, N., Dong, J., Zhu, B., Xu, B., Ma, Z. and Liu, J.: Recharge to the inter-dune
241 lakes and Holocene climatic changes in the Badain Jaran Desert, western China, *Quat.*
242 *Res.*, 73(1), 10–19, doi:10.1016/j.yqres.2009.10.009, 2010.

243 Zhan, L., Chen, J., Xu, Y., Xie, F. and Wang, Y.: Allogenic water recharge of groundwater in
244 the Erenhot wasteland of northern China, *J. Radioanal. Nucl. Chem.*, 311(3), 2015–2028,
245 doi:10.1007/s10967-017-5175-4, 2017.

246 Zhao, L., Xiao, H., Dong, Z., Xiao, S., Zhou, M., Cheng, G., Yin, L. and Yin, Z.: Origins of
247 groundwater inferred from isotopic patterns of the Badain Jaran Desert, Northwestern
248 China, *Ground Water*, 50(5), 715–725, doi:10.1111/j.1745-6584.2011.00895.x, 2012.

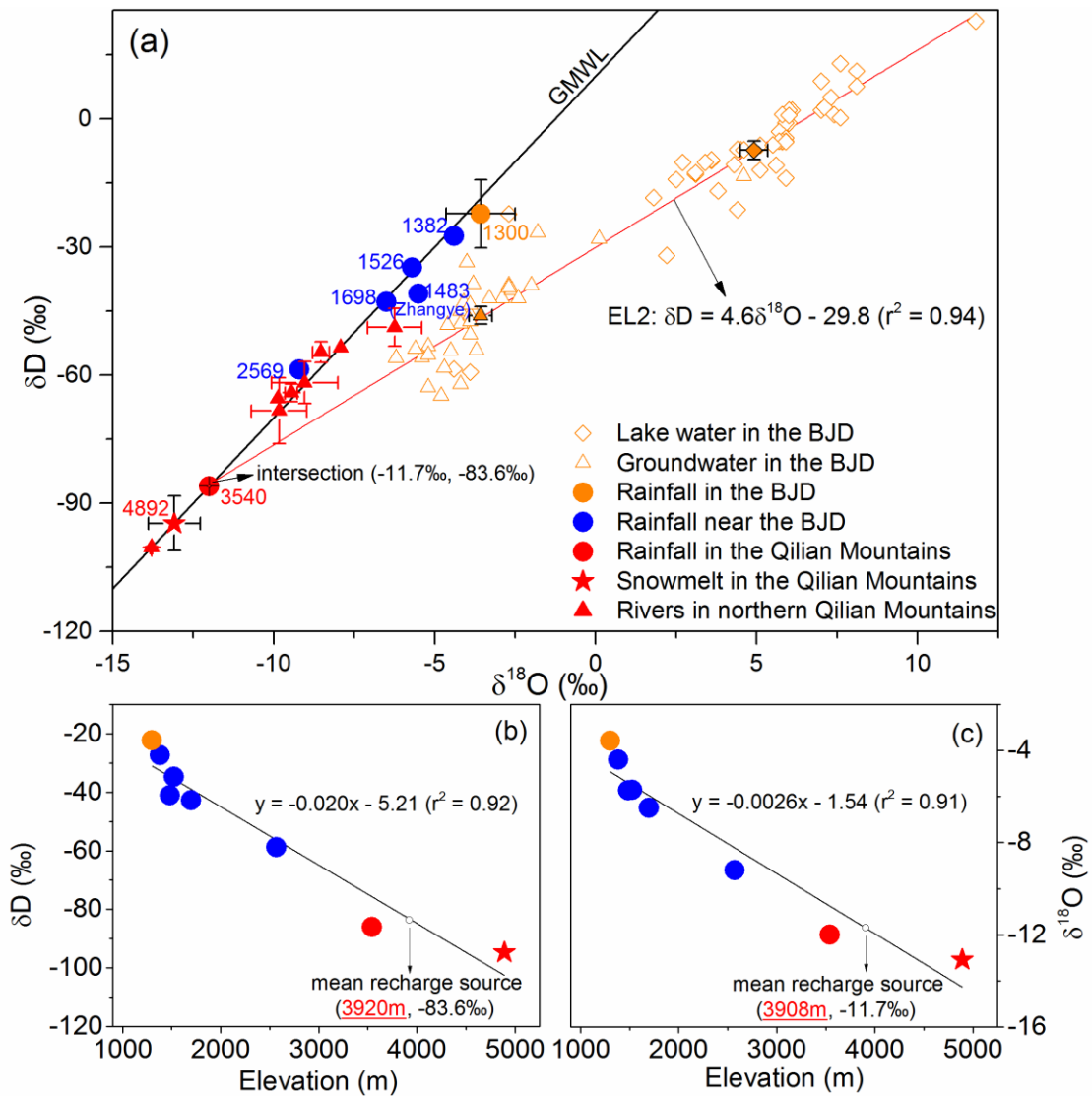
249 Zhu, G. F., Su, Y. H. and Feng, Q.: The hydrochemical characteristics and evolution of
250 groundwater and surface water in the Heihe River Basin, northwest China, *Hydrogeol. J.*,
251 16(1), 167–182, doi:10.1007/s10040-007-0216-7, 2008.

252



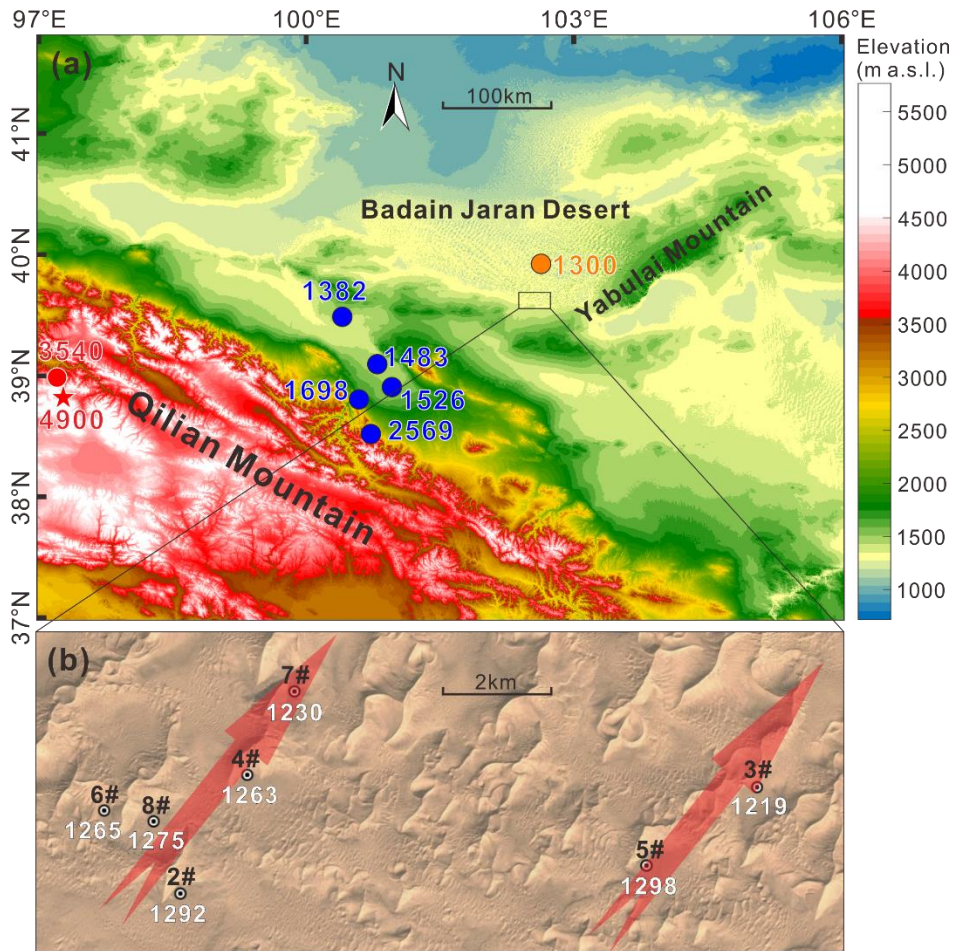
253

254 **Figure 1.** Isotope composition of monthly precipitation of the GNIP station Zhangye (all
 255 available datasets **(a)** and monthly mean values **(b)**), and δD - $\delta^{18}O$ plots of groundwater, lake
 256 water and annual precipitation in the study area (based on data from Zhangye station) **(c)**. Data
 257 in **(a)** and **(b)** are sourced from the GNIP database while plot **(c)** is modified from Wu et al.
 258 (2017). Statistical mean values are shown together with standard errors where feasible.



259

260 **Figure 2.** δD vs. $\delta^{18}O$ plot of water related to the BJD groundwater origin (a), and altitude
 261 gradients of related precipitation isotopes (b, c). For precipitation (rainfall and snowmelt), the
 262 corresponding sampling elevations (m a.s.l.) are also shown. Statistical mean values are shown
 263 together with standard errors where feasible. The weighted means of local rainfall (blue circles)
 264 are from Wu et al. (2010) and the GNIP database. Rainfall (yellow circle), lake water (yellow
 265 square; 47 samples) and groundwater (yellow triangle; 31 samples) in within the BJD area are
 266 based on data from Wu et al. (2017), Ma and Edmunds (2006), Zhao et al. (2012), Gates et al.
 267 (2008), Chen et al. (2012) and Yang et al. (2010). Summer rainfall (red circle; 4 samples) and
 268 snowmelt (red pentagram; 15 samples) in the Qilian Mountains are based on data from Ren
 269 (1999). Isotopic data for various rivers (red triangles) on the northern slope of the Qilian
 270 Mountain are collected from Chen et al. (2012), Li et al. (2016), Zhu, Su, and Feng (2008) and
 271 Ren (1999).



272

273 **Figure 3.** Elevation map of the Qilian Mountains and BJD areas **(a)** and groundwater wells
 274 drilled in the BJD **(b)**. Locations for precipitation sampling in different areas are also shown in
 275 **(a)**, as well as the elevation (m a.s.l.). The elevations of static groundwater levels in seven of
 276 the extraction wells (well #1 is far away from these wells and hence not shown) are indicated
 277 by white text in **(b)**. Arrows in **(b)** show the estimated groundwater flow direction (based on
 278 groundwater elevation).